THE JOURNAL OF PHYSICAL CHEMISTRY A

Article

pubs.acs.org/JPCA

Energy-Transfer Kinetics Driven by Midinfrared Amplified Spontaneous Emission after Two-Photon Excitation from Xe (s_0) to the Xe ($6p[1/2]_0$) State

Shan He,[†,‡] Yafu Guan,[‡,§] Dong Liu,[†,‡] Xusheng Xia,[†,‡] Baodong Gai,[†,‡] Shu Hu,[†] Jingwei Guo,*[,†] Fengting Sang,[†] and Yuqi Jin[†]

[†]Key Laboratory of Chemical Lasers, Dalian Institute of Chemical Physics, Chinese Academy of Sciences, Dalian 116023, P. R. China

[‡]University of Chinese Academy of Sciences, Beijing 100049, P. R. China

[§]State Key Laboratory of Molecular Reaction Dynamics, Dalian Institute of Chemical Physics, Chinese Academy of Sciences, Dalian 116023, P. R. China

ABSTRACT: In optically pumped laser systems, rare gas lasers (RGLs) are a field of great interest for researchers. Gas laser regimes with metastable Ne, Ar, and Kr atoms have been investigated, while studies of RGLs based on metastable Xe are sparse. In this work, when a strong excitation laser (2.92 mJ/pulse, 7.44×10^5 W/cm^2) was applied to excite Xe atoms from the ground state to the $6p[1/2]_0$ state, an interesting phenomenon emerged: An intense fluorescence of 980 nm ($6p[1/2]_1$–$6s[3/2]_2$) was produced. However, when the energy of excitation laser was decreased to 0.50 mJ/pulse (1.27×10^5 W/cm^2), the fluorescence of 980 nm became very weak. Besides, lifetime and decay rate constant of the $6p[1/2]_0$ state under the condition of E = 2.92 mJ are significantly different from either those measured by other groups or those of E = 0.50 mJ. These phenomena indicate that the high energy of excitation laser should trigger some new kinetic mechanisms. Further works identified that the new kinetic mechanism is the MIR ASE of 3408 nm ($6p[1/2]_0$–$6s'[1/2]_1$). The mechanisms are proposed as follows. Substantial $6p[1/2]_0$ atoms are produced by laser excitation. Then, the ASE of 3408 nm ($6p[1/2]_0$–$6s'[1/2]_1$) is quickly produced to populate substantial $6s'[1/2]_1$ atoms. The $6s'[1/2]_1$ atoms can readily arrive at the $6p[1/2]_1$ states through collision by virtue of the small energy difference (84 cm^{-1}) and high collision rate constant of the transition from the $6s'[1/2]_1$ state to the $6p[1/2]_1$ state. As a result, the intense fluorescence of 980 nm is generated.

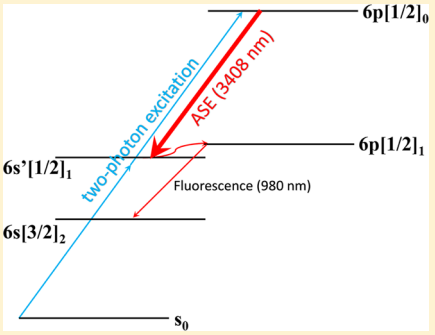

INTRODUCTION

Recently, there have been enormous efforts to develop high-energy optically pumped alkali vapor lasers (DPAL),[1−4] due to their excellent beam quality, high quantum efficiency, and high gain coefficient. However, many challenges still remain. The windows of the cell are easily destroyed by alkali metal vapors. In addition, to fulfill population inversion, hydrocarbons, such as methane and ethane, are often added into the system. Alkali metal vapors can react with the hydrocarbons slowly.[5,6] Therefore, the lifetime of the cell containing alkali vapor is seriously reduced.

A new class of optically pumped laser system, rare gas laser (RGL),[7] was proposed as an alternative for DPAL because the electric configurations of metastable rare gas atoms are similar to those of alkali metal atoms. The long-lifetime $np^5(n+1)s$ states of rare gas atoms are readily populated under mild electric discharge conditions. Therefore, they can potentially be used as the lower levels of the laser. Many groups have studied this new system.[8−17] Heaven and coworkers have studied RGL laser systems with the metastable states of Ne, Ar, and Kr,[8−13] and they successfully produced a continuous-wave (CW) optically pumped Ar laser. Rawlins and coworkers obtained high Ar ($5s[3/2]_2$) concentrations and optical efficiency (55%) by applying microdischarge arrays.[14,15] Wang and coworkers proposed a modeling of diode pumped metastable rare gas lasers,[16] which is helpful for the rational design of high efficient RGL.

The metastable states of Xe are easier to prepare than those of lighter rare gases. However, studies based on metastable Xe are relatively rare. Many groups have studied the energy-transfer processes between the high excitation states of Xe.[18−29] However, the excitation energies they used are lower than the threshold of the mid-infrared ASE.

In this work, when a strong excitation laser (2.92 mJ/pulse, 7.44×10^5 W/cm^2) was applied to excite Xe atoms from ground state to the $6p[1/2]_0$ state, an intense fluorescence of 980 nm ($6p[1/2]_1$–$6s[3/2]_2$) was produced. These should be owed to a new kinetic process. Further works proved that the new process is the MIR amplified spontaneous emission (ASE). Because the intensity of fluorescence of 980 nm ($6p[1/2]_1$–$6s[3/2]_2$) is pretty strong, the $6p[1/2]_0$ atoms tend to decay through the ASE of 3408 nm ($6p[1/2]_0$–$6s'[1/2]_1$). Therefore,

Received: February 27, 2017
Revised: April 21, 2017
Published: April 25, 2017

DOI: 10.1021/acs.jpca.7b01905
J. Phys. Chem. A 2017, 121, 3430−3436

metastable Xe atoms may be a potential medium for MIR laser. The electronic states of Xe relevant to this work are illustrated in Figure 1.

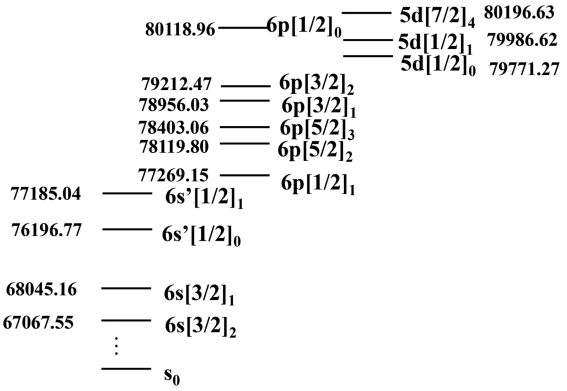

Figure 1. Schematic diagram of the energy levels of Xe* related to this work. Each state is marked with its energy (in cm^{-1}) in reference to the ground state s_0. The Racah notation is used throughout this article.

EXPERIMENTAL METHODS

A schematic diagram of the experimental apparatus used in this work is shown in Figure 2. A stainless-steel cell with four windows (L = 145 mm, d = 35 mm) was used to contain the ultrahigh purity Xe (99.999%). One window of the cell is made of sapphire. The others are made of fused quartz. The third harmonic of a Nd:YAG laser (Beamtech SGR-10) was used to pump a dye laser (Sirah CBST-LG-18-EG). The repetition rate of the laser system was 10 Hz. Coumarin 307 was applied to tune the laser in the range from 480 to 540 nm. This tunable laser passed through a BBO crystal to produce a tunable ultraviolet (UV) laser. The UV laser was separated from the fundamental laser by a series of Pellin-Broca prisms and has a full width at half maximum (fwhm) of ~7 ns. The beam diameter of the excitation laser is 5.0 mm. The Xe ($6p[1/2]_0$, $6p[3/2]_2$, and $6p[5/2]_2$) atoms were prepared by two-photon excitation at wavelengths about 249.5, 252.4, and 255.9 nm, respectively. The energies of the excitation pulse were monitored by a power meter (Gentec QE 12LP-S-MB-D0). The pressures of the gas were measured by a UNIK 5000 manometer.

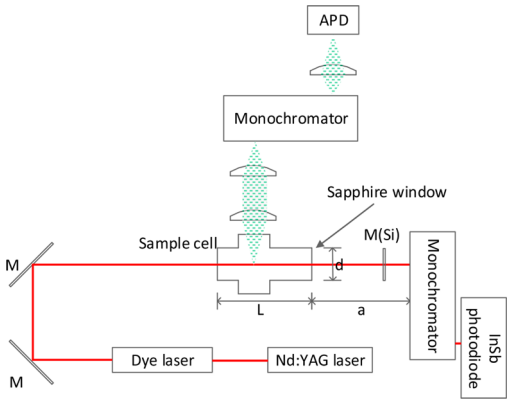

Figure 2. Schematic diagram of the experimental apparatus.

The fluorescence was collected along the axis perpendicular to the excitation laser by a lens system. A monochromator (Princeton Instrument SpectraPro 2500i) with a 1200 g/mm grating was used to disperse the different spontaneous emission spectral lines. The specific spontaneous emission line was focused by a lens and detected by an avalanche photodiode (APD 430A). The response range of the APD is from 400 to 1000 nm, and the maximum response is at ~820 nm. The intensities of spontaneous emissions are all within the linear response range of this APD. The output signals of the APD were digitized and recorded by a 2 GHz oscilloscope (LeCroy waverunner 620zi). Typically, 200 laser shots were averaged to ensure a good signal-to-noise ratio.

In the forward direction along the laser axis, an uncoated Si plate was used to absorb the excitation laser and transmit the MIR ASE. A monochromator (HORIBA micro HR MHRA-2A-MS) with a 300 g/mm infrared grating was used to disperse the ASE signals. The intensities of the MIR ASE were detected by a photodiode (InSb). To avoid the interference of the divergence angle of ASE, the distance between the sapphire window and the monochromator was set to 20 cm (a = 20 cm), and a series of apertures were placed between the sapphire window and the monochromator.

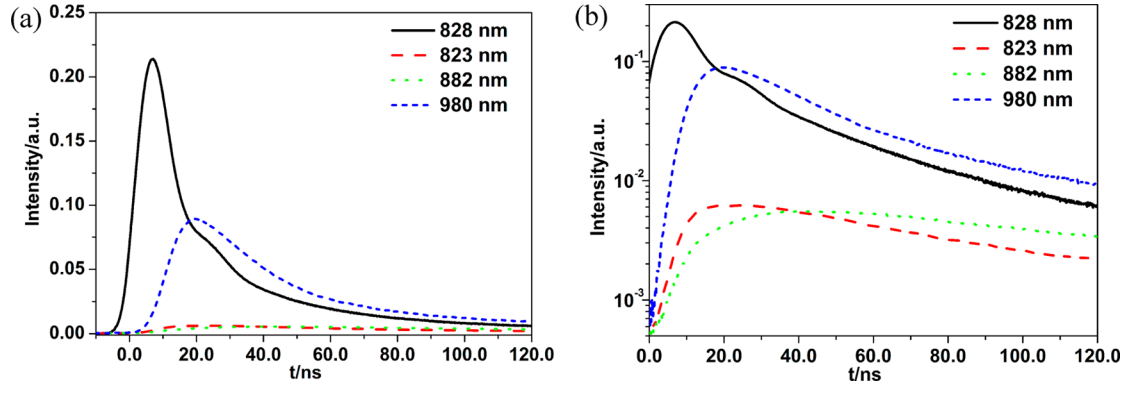

Figure 3. Time-resolved fluorescence curves after two-photon excitation of Xe atoms from the ground state to the $6p[1/2]_0$ state. (a,b) Plotted on linear and semilogarithmic scale, respectively. The energy of excitation laser is 2.92 mJ (7.44×10^5 W/cm^2). These plots were acquired in 10.8 Torr of Xe. The $6p[1/2]_0$ atoms are produced by laser excitation. The $6p[3/2]_2$, $6p[5/2]_3$, and $6p[1/2]_1$ states are secondary states. Note: 828 nm ($6p[1/2]_0$–$6s[3/2]_1$); 980 nm ($6p[1/2]_1$–$6s[3/2]_2$); 882 nm ($6p[5/2]_3$–$6s[3/2]_2$); 823 nm ($6p[3/2]_2$–$6s[3/2]_2$).

DOI: 10.1021/acs.jpca.7b01905
J. Phys. Chem. A 2017, 121, 3430–3436

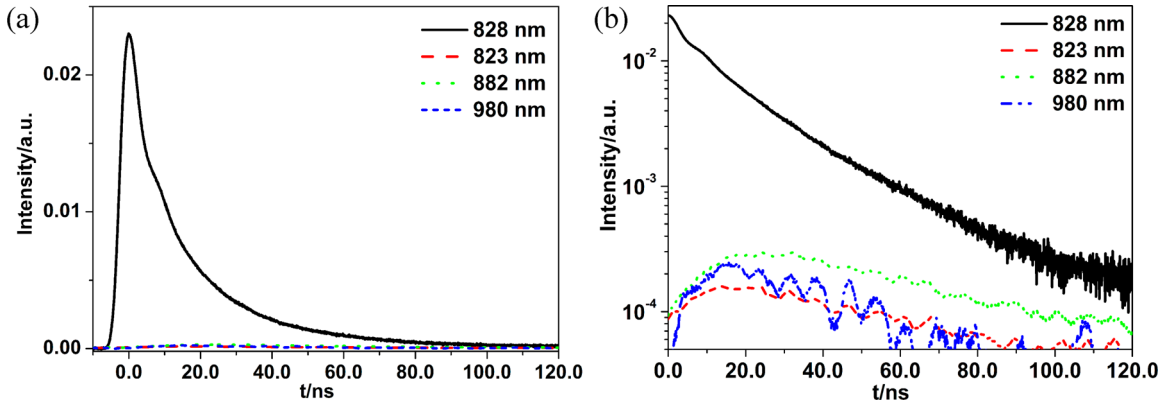

Figure 4. Time-resolved fluorescence curves after two-photon excitation of Xe atoms from the ground state to the $6p[1/2]_0$ state. (a,b) Plotted on linear and semilogarithmic scale, respectively. The energy of excitation laser is 0.50 mJ (1.27×10^5 W/cm^2). The other conditions are the same as those of Figure 3.

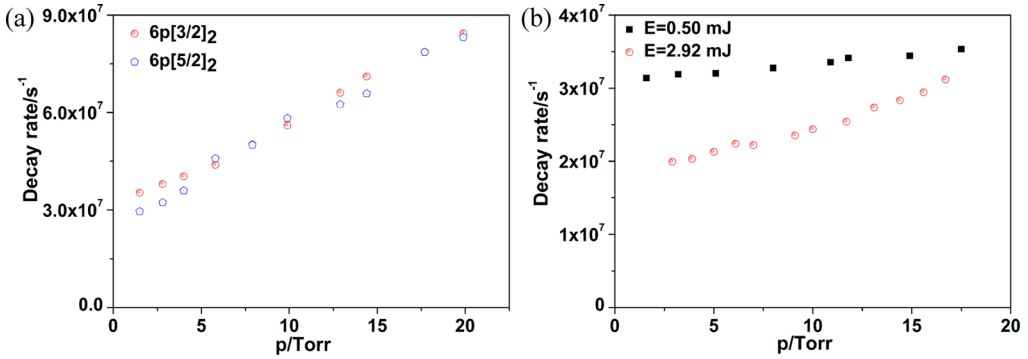

Figure 5. (a) Pressure dependence of the total decay rates of the $6p[3/2]_2$ and $6p[5/2]_2$ states of Xe. The points in this plot were fitted from the time-resolved fluorescence curves under the condition of E = 0.50 mJ. (b) Pressure dependence of the total decay rates of the $6p[1/2]_0$ state of Xe. The points in this plot were obtained under the conditions of E = 2.92 and 0.50 mJ. These three states are all prepared by two-photon excitation of ground-state Xe atoms. The wavelengths of the excitation laser are ~249.5 nm for $6p[1/2]_0$, 252.4 nm for $6p[3/2]_2$, and 255.9 nm for $6p[5/2]_2$, respectively.

RESULTS AND DISCUSSION

When a strong laser (2.92 mJ/pulse, 7.44×10^5 W/cm^2) was applied to prepare Xe ($6p[1/2]_0$) atoms, the time-resolved fluorescence spectra were observed and are shown in Figure 3. The fluorescence of 828 nm ($6p[1/2]_0$–$6s[3/2]_1$) is the most intense because the $6p[1/2]_0$ atoms are produced by laser excitation directly. Unexpectedly, a very intense spontaneous emission of 980 nm ($6p[1/2]_1$–$6s[3/2]_2$) was also observed. This implies that substantial atoms are populated in the $6p[1/2]_1$ state. Therefore, $6p[1/2]_0$ atoms have high probability of arriving at the $6p[1/2]_1$ state. The fluorescence spectra of the excited states of Xe have been studied,[18,28] but the spontaneous emission of 980 nm by exciting of Xe from the ground state to the $6p[1/2]_0$ state has never been reported before. The major difference between our work and previous literatures is that the energy of excitation laser is relatively high. Therefore, the high energy of excitation laser is suspected to trigger the intense fluorescence of 980 nm ($6p[1/2]_1$–$6s[3/2]_2$). To prove the assumption, these fluorescences were measured again under the condition of E = 0.50 mJ (1.27×10^5 W/cm^2). The results are shown in Figure 4.

As expected, the intensity of fluorescence of 980 nm ($6p[1/2]_1$–$6s[3/2]_2$) is very weak in Figure 4. The high energy of excitation laser should trigger some new kinetic processes to populate substantial $6p[1/2]_1$ atoms. Besides, the total decay rate of the $6p[1/2]_0$ state in Figure 3 seems different from that shown in Figure 4. The high energy of excitation laser may also influence the kinetic parameters. Therefore, the kinetic parameters of the Xe($6p[1/2]_0$) state under conditions of high and low energy of excitation laser are studied. First, as a benchmark work, kinetic parameters of $6p[3/2]_2$ and $6p[5/2]_2$ states of Xe were calculated and fitted from the time-resolved fluorescence spectra of 823 nm ($6p[3/2]_2$–$6s[3/2]_2$) and 904 nm ($6p[5/2]_2$–$6s[3/2]_2$), respectively. These time-resolved curves for fitting were obtained when these two states were directly prepared by laser.

The $6p[3/2]_2$ state is taken as an example to illustrate the details of calculation model. Because only the declining part of the fluorescence curve is used for fitting and calculation, the kinetic processes are decay channels of relaxation and radiation. Then, the decay processes can be depicted by formula 1

$$\frac{\mathrm{d}[6p[3/2]_2]}{\mathrm{d}t} = -(k_{6p[3/2]_2,\mathrm{Xe}}[\mathrm{Xe}] + k_{6p[3/2]_2,\mathrm{r}})[6p[3/2]_2] \quad (1)$$

where $k_{6p[3/2]_2,\mathrm{Xe}}[\mathrm{Xe}]$ is the collision decay rate of Xe; $k_{6p[3/2]_2,\mathrm{Xe}}$ is the collision decay rate constant of Xe, which only depends on temperature; $k_{6p[3/2]_2,\mathrm{r}}$ is the radiative decay rate; and $[6p[3/2]_2]$ is the relative population of the $6p[3/2]_2$ state. It is easy to deduce formula 2 from formula 1.

$$[6p[3/2]_2] = [6p[3/2]_2]_0 \mathrm{e}^{-Kt} \quad (2)$$

DOI: 10.1021/acs.jpca.7b01905
J. Phys. Chem. A 2017, 121, 3430–3436

Table 1. Total Decay Rate Constants and Lifetimes of the $6p[1/2]_0$, $6p[3/2]_2$, and $6p[5/2]_2$ States[a]

states		$6p[1/2]_0$		$6p[3/2]_2$	$6p[5/2]_2$
total decay rate constant/10^{-11} cm^{-3} s^{-1}	this work	2.32 ± 0.11 (2.92 mJ)	0.73 ± 0.04 (0.50 mJ)	8.27 ± 0.19	8.20 ± 0.39
	ref 18	0.58 ± 0.05		8.2 ± 0.5	9.6 ± 0.3
	ref 28	0.59 ± 0.05		10.1 ± 0.03	11.6 ± 0.03
	ref 29			8.7 ± 0.8	10.1 ± 0.5
lifetime/ns	this work	58.3 ± 1.5 (2.92 mJ)	32.3 ± 0.1 (0.50 mJ)	33.8 ± 0.9	38.8 ± 2.3
	ref 18	32.6 ± 1.0		36.0 ± 3.0	39.3 ± 1.0
	ref 28	26.8 ± 0.8		31.3 ± 1.8	36.0 ± 2.8

[a]In this Table, those parameters of the $6p[1/2]_0$ state were fitted from the time-resolved fluorescence curves under the conditions of E = 2.92 and 0.50 mJ. The parameters of the $6p[3/2]_2$ and $6p[5/2]_2$ states were fitted from the time-resolved fluorescence curves under the condition of E = 0.50 mJ.

where K is the total decay rate and $K = k_{6p[3/2]_2,Xe}[Xe] + k_{6p[3/2]_2,r}$. To avoid the influence of the dark current, a parameter "b" is added in the fitting function. Then, the fitting function can be expressed as formula 3.

$$[6p[3/2]_2] = [6p[3/2]_2]_0 e^{-Kt} + b \quad (3)$$

Approximately 15 ns after the laser pulse was terminated, the declining parts of the curve of the fluorescence of 823 nm ($6p[3/2]_2$–$6s[3/2]_2$) were fitted by formula 3. The total decay rates, "K", versus various Xe pressures (referred to as Stern–Volmer plot) are plotted in Figure 5a. A linear function was used to fit the points in Figure 5a. Then, the slope is the total decay rate constant, and the reciprocal of the intercept is the lifetime. When the $6p[5/2]_2$ state is prepared directly by laser, it has the similar mechanism to decay. So the kinetic parameters of the $6p[5/2]_2$ state can also be deduced by the above method. The Stern–Volmer plot of the $6p[5/2]_2$ state is also plotted in Figure 5a. All calculation results are listed in Table 1. The kinetic parameters of these two states are approximately in agreement with the parameters measured by previous literatures. Then, the lifetime and decay rate constant of the $6p[1/2]_0$ state under the condition of E = 2.92 and 0.50 mJ were fitted and calculated by the same method above. The Stern–Volmer plot is shown in Figure 5b, and the calculation results are also listed in Table 1.

As shown in Table 1, when the energy of excitation laser is 2.92 mJ, the kinetic parameters of the $6p[1/2]_0$ state are significantly different from either those of E = 0.50 mJ or those measured by other groups. Combining with the intense fluorescence of 980 nm shown in Figure 3, there must be some new kinetic mechanisms accelerating the transition from the $6p[1/2]_0$ state to the $6p[1/2]_1$ state under the condition of high energy of excitation laser. The energy difference between the $6p[1/2]_0$ and $6p[1/2]_1$ states is ~2849 cm^{-1}. The probability of direct relaxation from the $6p[1/2]_0$ to $6p[1/2]_1$ state by collision is very small. The cascade relaxation via states of $6p[3/2]_2$ and $6p[5/2]_3$ and so on is possible. The decay rate constants (by collision) of the $6p[3/2]_2$ and $6p[5/2]_3$ states are 8.27×10^{-11} (this work) and 5.3×10^{-11} cm^{-3} s^{-1} (ref 18), respectively. Then, the decay rates (by collision) of the $6p[3/2]_2$ and $6p[5/2]_3$ states under the condition of the p_{Xe} = 10.8 Torr are 2.99×10^7 and 1.92×10^7 s^{-1}, respectively. In addition, the radiative decay rates of the $6p[3/2]_2$ and $6p[5/2]_3$ states are 2.96×10^7 (this work) and 3.096×10^7 s^{-1} (ref 18), respectively. The radiation and collision decay rates are in the similar level. Therefore, radiative probabilities of these two states are pretty high, but the intensities of fluorescences of 823 nm ($6p[3/2]_2$–$6s[3/2]_2$) and 882 nm ($6p[5/2]_3$–$6s[3/2]_2$) are much weaker than that of 980 nm ($6p[1/2]_1$–$6s[3/2]_2$) shown in Figure 3. Furthermore, if the $6p[1/2]_1$ atoms are produced by cascade relaxation, fluorescences of 823 nm ($6p[3/2]_2$–$6s[3/2]_2$) and 882 nm ($6p[5/2]_3$–$6s[3/2]_2$) should appear earlier than that of 980 nm ($6p[1/2]_1$–$6s[3/2]_2$), but the actual situation shown in Figure 3 is different. The rising edge of the 980 nm is earlier and quicker than that of 882 nm. So the cascade collision relaxation could not be the primary channel to produce substantial $6p[1/2]_1$ atoms. The processes seem to have a threshold. Therefore, two mechanisms are proposed to explain the processes. One possible mechanism is the Hyper-Raman. The laser may excite the Xe atoms to a virtual state near the $6p[1/2]_0$ state, then the stimulated Stokes laser (from the virtual state near the $6p[1/2]_0$ state to the $6p[1/2]_1$ state) is generated quickly to produce substantial $6p[1/2]_1$ atoms. The other possible mechanism is the amplified spontaneous emission (ASE). The ASE always leads to substantial increase in population of the lower state.[25]

To identify the mechanism about Hyper-Raman, excitation spectra of the $6p[1/2]_0$ and $6p[1/2]_1$ states are plotted in Figure 6. The intensities of fluorescences of 828 nm ($6p[1/2]_0$–$6s[3/2]_1$) and 980 nm ($6p[1/2]_1$–$6s[3/2]_2$) can reflect the populations in the $6p[1/2]_0$ and $6p[1/2]_1$ states, respectively. More intense fluorescence implies higher population in the upper state of the emission. The intensities of these two fluorescences were measured with different wavelengths of excitation laser. The energy of the excitation laser is 2.92 mJ. Then, these data were normalized. The excitation spectra of these two states were obtained. If the $6p[1/2]_1$ atoms are produced by Hyper-Raman mechanism, then the kinetic

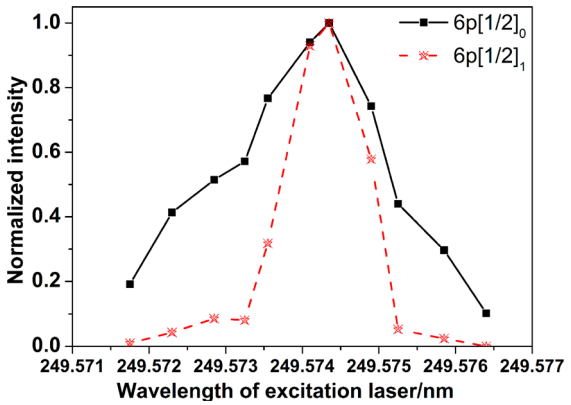

Figure 6. Excitation spectra of the $6p[1/2]_0$ and $6p[1/2]_1$ states. The energy of excitation laser is 2.92 mJ. The $6p[1/2]_0$ state is the laser-prepared state.

DOI: 10.1021/acs.jpca.7b01905
J. Phys. Chem. A 2017, 121, 3430–3436

process should be that laser excites the ground-state atoms to the virtual state near the $6p[1/2]_0$ state. Then, the stimulated Stokes laser (from the virtual state near the $6p[1/2]_0$ state to the $6p[1/2]_1$ state) is generated quickly to produce substantial $6p[1/2]_1$ atoms. Therefore, the excitation spectrum of the $6p[1/2]_1$ state should be broader than that of the $6p[1/2]_0$ state, especially in the red wing.[30] However, the excitation spectrum of the $6p[1/2]_1$ state is narrower than that of the $6p[1/2]_0$ state. Furthermore, Hyper-Raman radiation normally synchronizes with pump (excitation) laser in time-domain. So if the transition is due to Hyper-Raman mechanism, then the $6p[1/2]_0$ and $6p[1/2]_1$ states should be populated at the same time. Consequently, fluorescences of 828 and 980 nm should approximately start at the same time. Obviously, fluorescence of 828 nm starts earlier than fluorescence of 980 nm, as shown in Figure 3. Therefore, the possibility of Hyper-Raman mechanism is eliminated, and the mechanism is very likely to be ASE.

To further prove ASE mechanism, the following experiments were carried out. The radiation signals in the forward direction along the laser axis were detected when the $6p[1/2]_0$ state was the laser-prepared state. The spectrum was shown in Figure 7.

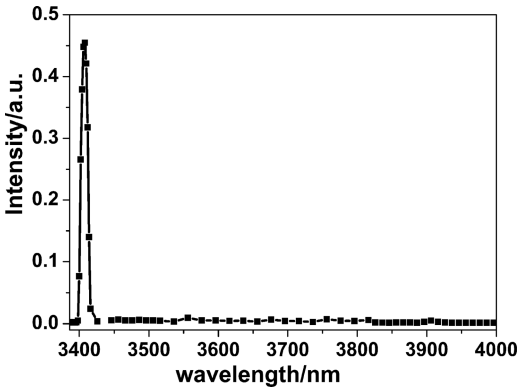

Figure 7. ASE spectrum in the forward direction along the laser axis. The $6p[1/2]_0$ state is the laser-prepared state. The energy of excitation laser is 2.92 mJ. The pressure of Xe is 10.8 Torr.

The wavelength of this ASE is 3408 nm, exactly corresponding to the atomic line of $6p[1/2]_0$–$6s'[1/2]_1$. The fwhm of this ASE is ~10 nm, and it may be due to the poor resolution of the IR monochromator used in this experiment. The fwhm of Nd:YAG (0.1 nm) laser recorded by this IR monochromator is also ~10 nm. Therefore, this ASE should be attributed to the atomic line of $6p[1/2]_0$–$6s'[1/2]_1$ (3408 nm). This ASE can generate substantial $6s'[1/2]_1$ atoms. The energy difference between the $6s'[1/2]_1$ and $6p[1/2]_1$ state is only ~84 cm^{-1}. Such a small energy difference can be readily crossed by collision. To further prove the relationship between the ASE of 3408 nm and the fluorescence of 980 nm, these signals were detected under the condition of different energies of excitation laser. The results are shown in Figure 8.

The thresholds of the ASE of 3408 nm ($6p[1/2]_0$–$6s'[1/2]_1$) and the spontaneous emission of 980 nm ($6p[1/2]_1$–$6s[3/2]_2$) are both ~1.5 mJ (3.82×10^5 W/cm^2). Only when the ASE of 3408 nm ($6p[1/2]_0$–$6s'[1/2]_1$) is produced can the spontaneous emission of 980 nm ($6p[1/2]_1$–$6s[3/2]_2$) be detected. Therefore, it is reasonable to conclude that the ASE of 3408 nm is the primary process to yield substantial $6p[1/2]_1$ atoms. The primary kinetic processes of $6p[1/2]_0 \rightarrow 6p[1/2]_1$,

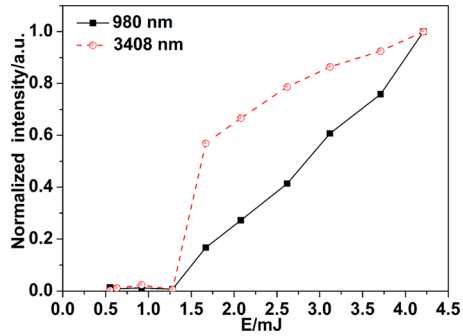

Figure 8. Dependence of normalized intensities of the spontaneous emission of 980 nm and ASE of 3408 nm on the energies of the excitation laser. All of these data were detected in 10.8 Torr Xe. The lines between the points are for easy reading only.

under the condition of E = 2.92 mJ (7.44×10^5 W/cm^2) and p = 10.8 Torr, can be described concisely by eqs 4–7.

$$Xe(s_0) \xrightarrow{\text{laser}} Xe(6p[1/2]_0) \quad (4)$$

$$Xe(6p[1/2]_0) \xrightarrow{\text{ASE(3408 nm)}} Xe(6s'[1/2]_1) \quad (5)$$

$$Xe(6s'[1/2]_1) + Xe(s_0) \xrightarrow{\text{collision}} Xe(6p[1/2]_1) + Xe(s_0) \quad (6)$$

$$Xe(6p[1/2]_1) \xrightarrow{\text{fluorescence (980 nm)}} Xe(6s[3/2]_2) \quad (7)$$

CONCLUSION

Once the energy of excitation laser is above a threshold of 1.5 mJ (3.82×10^5 W/cm^2) in the process of two-photon excitation from Xe (s_0) to the Xe ($6p[1/2]_0$) state, a new microscopic process, MIR ASE of 3408 nm ($6p[1/2]_0$–$6s'[1/2]_1$), can be triggered. This leads to substantial $6s'[1/2]_1$ atoms populated. Although the lifetime of the $6s'[1/2]_1$ state is only 3 to 4 ns[31] and the transfer from the $6s'[1/2]_1$ to $6p[1/2]_1$ state is an endothermic process, radiation trapping extends the apparent lifetime of the state to ~7.5 μs.[32] In addition, the tendency of the transfer from the $6s'[1/2]_1$ to $6p[1/2]_1$ state is pretty strong. The total relaxation rate constant of the $6s'[1/2]_1$ state is as high as $(6.65 \pm 1.00) \times 10^{-11}$ cm^3/s, and at least 75% of the relaxation is a transfer of population to the $6p[1/2]_1$ state.[32] Therefore, substantial $6p[1/2]_1$ atoms can be readily yielded by collision. As a result, the intense spontaneous emission of 980 nm ($6p[1/2]_1$–$6s[3/2]_2$) can be observed along the axis perpendicular to the excitation laser.

Lifetime and decay rate constant of the $6p[1/2]_0$ state are obviously changed when the energy of excitation laser is 2.92 mJ. This may result from two aspects. First, the high energy of excitation laser can trigger the ASE of 3408 nm ($6p[1/2]_0$–$6s'[1/2]_1$). The MIR ASE is an additional decay channel. Therefore, the lifetime should decrease and decay rate constant should increase. Second, many $6p[1/2]_0$ atoms may transfer to the $5d[1/2]_1$ states by collision for the small energy difference (132 cm^{-1}) between these two states.[33] The MIR ASE of 3408 nm ($6p[1/2]_0$–$6s'[1/2]_1$) can cause significant decrease in the population in the $6p[1/2]_0$ state. The inflection in the Figure 3a may be owed to this aspect. Then, the transition from the $5d[1/2]_1$ state to the $6p[1/2]_0$ state may play an important role in the decay process of the fluorescence of 828 nm. The lifetime of the $5d[1/2]_1$ state is ~4.9 μs.[33] Consequently, the lifetime of

DOI: 10.1021/acs.jpca.7b01905
J. Phys. Chem. A 2017, 121, 3430–3436

the $6p[1/2]_0$ state should increase. The change of kinetic parameters of the $6p[1/2]_0$ state shown in Table 1 may be owed to the combined effects of these two aspects. To prove this assumption, the time-resolved MIR ASE of 3408 nm ($6p[1/2]_0$–$6s'[1/2]_1$) on nanosecond scale and the time-resolved fluorescence spectrum of 3680 nm ($5d[1/2]_1$–$6p[1/2]_1$) are required. However, either of them is difficult to obtain due to the limitation of response time and sensitivity of our MIR detector. A detailed mechanism still needs to be further studied.

Because the fluorescence intensity of 980 nm ($6p[1/2]_1$–$6s[3/2]_2$) is very strong, the $6p[1/2]_0$ atoms tend to decay by the ASE radiations. In fact, ASE implies the induced emission in a medium with a high gain. Therefore, this optically pumped laser system can have quite high photon efficiency. This property indicates that metastable Xe may be a potential laser medium for MIR laser.

AUTHOR INFORMATION

Corresponding Author

*E-mail: jingweiguo@dicp.ac.cn.

ORCID

Jingwei Guo: 0000-0001-9158-7828

Notes

The authors declare no competing financial interest.

ACKNOWLEDGMENTS

This work is supported by the National Natural Science Foundation of China (Grant Nos. 11304311, 11475177, 61505210) and Key Laboratory of Chemical Laser Foundation (KLCL 2016).

REFERENCES

(1) Beach, R. J.; Krupke, W. F.; Kanz, V. K.; Payne, S. A.; Dubinskii, M. A.; Merkle, L. D. End-pumped Continuous-wave Alkali Vapor Lasers: Experiment, Model, and Power Scaling. *J. Opt. Soc. Am. B* **2004**, *21*, 2151–2163.

(2) Readle, J. D.; Wagner, C. J.; Verdeyen, J. T.; Spinka, T. M.; Carroll, D. L.; Eden, J. G. *Excimer-Pumped Alkali Vapor Lasers: A New Class of Photoassociation Lasers*, Conference on High Energy/Average Power Lasers and Intense Beam Applications IV, SPIE, Jan 25–26, 2010; Davis, S. J., Heaven, M. C., Schriempf, J. T., Eds.; San Francisco, CA, 2010.

(3) Li, Y.; Hua, W.; Li, L.; Wang, H.; Yang, Z.; Xu, X. Experimental Research of a Chain of Diode Pumped Rubidium Amplifiers. *Opt. Express* **2015**, *23*, 25906–25911.

(4) Moran, P. J.; Richards, R. M.; Rice, C. A.; Perram, G. P. Near Infrared Rubidium $6^2P_{3/2,1/2}$→$6^2P_{1/2}$ Laser. *Opt. Commun.* **2016**, *374*, 51–57.

(5) Tam, A.; Moe, G.; Happer, W. Particle Formation by Resonant Laser Light in Alkali-metal Vapor. *Phys. Rev. Lett.* **1975**, *35*, 1630–1633.

(6) Tanaka, T.; Mitsui, T.; Sugiyama, K.; Kitano, M.; Yabuzaki, T. Shapes of Laser-produced CsH Particles. *Phys. Rev. Lett.* **1989**, *63*, 1390–1392.

(7) Kabir, M. H.; Heaven, M. C. Energy Transfer Kinetics of the $np^5(n+1)p$ Excited States of Ne and Kr. *J. Phys. Chem. A* **2011**, *115*, 9724–9730.

(8) Han, J.; Heaven, M. C. Gain and Lasing of Optically Pumped Metastable Rare Gas Atoms. *Opt. Lett.* **2012**, *37*, 2157–2159.

(9) Han, J.; Glebov, L.; Venus, G.; Heaven, M. C. Demonstration of a Diode-pumped Metastable Ar Laser. *Opt. Lett.* **2013**, *38*, 5458–5461.

(10) Kabir, M. H.; Heaven, M. C. *Collisional Relaxation of the Kr ($4p^5 5p$) States in He, Ne, and Kr*, Conference on High Energy/Average Power Lasers and Intense Beam Applications IV Atmospheric and Oceanic Propagation of Electromagnetic Waves IV, SPIE, Jan 22–24, 2012; Davis, S. J., Heaven, M. C., Schriempf, J. T., Korotkova, O., Eds.; San Francisco, CA, 2012.

(11) Han, J.; Heaven, M. C. Kinetics of Optically Pumped Ar Metastables. *Opt. Lett.* **2014**, *39*, 6541–6544.

(12) Han, J.; Heaven, M. C.; Hager, G. D.; Venus, G. B.; Glebov, L. B. *Kinetics of an Optically Pumped Metastable Ar Laser*, Conference on High Energy/Average Power Lasers and Intense Beam Applications VII, SPIE, Feb 02–04, 2014; Davis, S. J., Heaven, M. C., Schriempf, J. T., Eds.; San Francisco, CA, 2014.

(13) Han, J.; Heaven, M. C. Kinetics of Optically Pumped Kr Metastables. *Opt. Lett.* **2015**, *40*, 1310–1313.

(14) Rawlins, W. T.; Galbally-Kinney, K. L.; Davis, S. J.; Hoskinson, A. R.; Hopwood, J. A. *Laser Excitation Dynamics of Argon Metastables Generated in Atmospheric Pressure Flows by Microwave Frequency Microplasma Arrays*, Conference on High Energy/Average Power Lasers and Intense Beam Applications VII, SPIE, Feb 02–04, 2014; Davis, S. J., Heaven, M. C., Schriempf, J. T., Eds.; San Francisco, CA, 2014.

(15) Rawlins, W. T.; Galbally-Kinney, K. L.; Davis, S. J.; Hoskinson, A. R.; Hopwood, J. A.; Heaven, M. C. Optically Pumped Microplasma Rare Gas Laser. *Opt. Express* **2015**, *23*, 4804–4813.

(16) Yang, Z.; Yu, G.; Wang, H.; Lu, Q.; Xu, X. Modeling of Diode Pumped Metastable Rare Gas Lasers. *Opt. Express* **2015**, *23*, 13823–13832.

(17) Mikheyev, P. A. Optically Pumped Rare-gas Lasers. *Quantum Electron.* **2015**, *45*, 704–708.

(18) Ku, J. K.; Setser, D. W. Collisional Deactivation of Xe ($5p^5 6p$) States in Xe and Ar. *J. Chem. Phys.* **1986**, *84*, 4304–4316.

(19) Horiguchi, H.; Chang, R. S. F.; Setser, D. W. Radiative Lifetimes and Two-body Collisional Deactivation Rate Constants in Ar for Xe ($5p^5 6p$), Xe ($5p^5 6p$), and Xe ($5p^5 7p$) States. *J. Chem. Phys.* **1981**, *75*, 1207–1218.

(20) Xu, J.; Setser, D. W. Collisional Deactivation Studies of the Xe (6p) States in He and Ne. *J. Chem. Phys.* **1991**, *94*, 4243–4251.

(21) Inoue, G.; Ku, J. K.; Setser, D. W. Laser Induced Fluorescence Study of Xe ($5p^5 6p$, $5p^5 6p'$, $5p^5 7p$, and $5p^5 6d$) States in Ne and Ar: Radiative Lifetimes and Collisional Deactivation Rate Constants. *J. Chem. Phys.* **1984**, *81*, 5760–5774.

(22) Xu, J.; Setser, D. W. Deactivation Rate Constants and Product Branching in Collisions of the Xe (6p) States with Kr and Ar. *J. Chem. Phys.* **1990**, *92*, 4191–4202.

(23) Nelson, T. O.; Setser, D. W.; Richmann, M. K. Quenching Rate Constants of the Xe ($5p^5 6p$ and $6p'$) States and the Energy-pooling Ionization Reaction of Xe ($5p^5 6s$) Atoms. *J. Phys. Chem.* **1995**, *99*, 7482–7494.

(24) Alekseev, V. A.; Setser, D. W. Quenching Rate Constants and Product Assignments for Reactions of Xe ($7p[3/2]_2$, $7p[5/2]_2$, and $6p'[3/2]_2$) Atoms with Rare Gases, CO, H_2, N_2O, CH_4, and Halogen-containing Molecules. *J. Phys. Chem.* **1996**, *100*, 5766–5780.

(25) Alekseev, V. A.; Setser, D. W. A Pulsed Source for Xe ($6s[3/2]_1$) and Xe ($6s'[1/2]_1$) Resonance State Atoms Using Two-photon Driven Amplified Spontaneous Emission from the Xe (6p) and Xe ($6p'$) States. *J. Chem. Phys.* **1996**, *105*, 4613–4625.

(26) Böwering, N.; Bruce, M. R.; Keto, J. W. Collisional Deactivation of Two-photon Laser Excited Xenon $5p^5 6p$. I. State-to-state Reaction Rates. *J. Chem. Phys.* **1986**, *84*, 709–714.

(27) Böwering, N.; Bruce, M. R.; Keto, J. W. Collisional Deactivation of Two-photon Laser Excited Xenon $5p^5 6p$. II. Lifetimes and Total Quench Rates. *J. Chem. Phys.* **1986**, *84*, 715–726.

(28) Bruce, M. R.; Layne, W. B.; Whitehead, C. A.; Keto, J. W. Radiative Lifetimes and Collisional Deactivation of Two-photon Excited Xenon in Argon and Xenon. *J. Chem. Phys.* **1990**, *92*, 2917–2926.

(29) Alford, W. J. State-to-state Rate Constants for Quenching of Xenon 6p Levels by Rare Gases. *J. Chem. Phys.* **1992**, *96*, 4330–4340.

(30) Cotter, D.; Hanna, D. C.; Tuttlebee, W. H. W.; Yuratich, M. A. Stimulated Hyper-Raman Emission from Sodium Vapour. *Opt. Commun.* **1977**, *22*, 190–194.

DOI: 10.1021/acs.jpca.7b01905
J. Phys. Chem. A 2017, 121, 3430–3436

(31) Anderson, D. K. Lifetime of $(5p^5 6s)^1p_1$ and $^3p_1$ States of Xenon. *Phys. Rev. A* **1965**, *137*, 21−26.
(32) Sadeghi, N.; Sabbagh, J. Collisional Transfer between the $6s'[1/2]_{0,1}$ and $6p[1/2]_1$ Xenon Levels. *Phys. Rev. A: At., Mol., Opt. Phys.* **1977**, *16*, 2336−2345.
(33) Museur, L.; Kanaev, A. V.; Zheng, W. Q.; Castex, M. C. Collisional Energy Transfer in Gaseous Xenon with Vacuum Ultraviolet Laser Excitation of the $5d[1/2]_1$ Atomic Level. *J. Chem. Phys.* **1994**, *101*, 10548−10558.

DOI: 10.1021/acs.jpca.7b01905
J. Phys. Chem. A 2017, 121, 3430−3436